Enhanced performances of InGaN/GaN-based blue light-emitting diode with InGaN/AlInGaN superlattice electron blocking layer*

Zhuo Xiang-Jing(卓祥景), Zhang Jun(章 俊), Li Dan-Wei(李丹伟), Yi Han-Xiang(易翰翔), Ren Zhi-Wei(任志伟), Tong Jin-Hui(童金辉), Wang Xing-Fu(王幸福), Chen Xin(陈 鑫), Zhao Bi-Jun(赵璧君), Wang Wei-Li(王伟丽), and Li Shu-Ti(李述体)†

Laboratory of Nano-photonic Functional Materials and Devices, Institute of Opto-electronic Materials and Technology, South China Normal University, Guangzhou 510631, *China*

(Received 29 September 2013; revised manuscript received 13 November 2013; published online 10 April 2014)

InGaN/AlInGaN superlattice (SL) is designed as the electron blocking layer (EBL) of an InGaN/GaN-based light-emitting diode (LED). The energy band structure, polarization field at the last-GaN-barrier/EBL interface, carrier concentration, radiative recombination rate, electron leakage, internal quantum efficiency (IQE), current–voltage (I–V) performance curve, light output–current (L–I) characteristic, and spontaneous emission spectrum are systematically numerically investigated using APSYS simulation software. It is found that the fabricated LED with InGaN/AlInGaN SL EBL exhibits higher light output power, low forward voltage, and low current leakage compared with those of its counterparts. Meanwhile, the efficiency droop can be effectively mitigated. These improvements are mainly attributed to the higher hole injection efficiency and better electron confinement when InGaN/AlInGaN SL EBL is used.

Keywords: light-emitting diode, InGaN/AlInGaN superlattice, efficiency droop

PACS: 85.60.Jb, 8715.A–, 78.60.Fi, 73.61.Ey **DOI:** 10.1088/1674-1056/23/6/068502

1. Introduction

Recently, solid-state lightings, especially InGaN/GaN-based light-emitting diodes (LEDs), have been vigorously developed to take the place of traditional lighting and display sources, due to their high efficiency and long lifetimes.[1] However, the reduction of emission efficiency at high injection current density, which is often dubbed "efficiency droop", seriously restricts the high-power, high-brightness applications of InGaN/GaN-based LEDs.[2] Various models for the efficiency droop have been proposed, including Auger recombination,[3,4] polarization-assisted electron leakage,[5,6] lack of hole injection,[7,8] defects,[9] and junction heating.[10] Among these factors, electron leakage out of the active region as well as inefficient hole injection have been identified to be the major reasons for efficiency droop.[11] To reduce the electron leakage, $Al_XGa_{1-X}N$ electron blocking layer (EBL) is often adopted between the last quantum barrier (QB) layer and the p-GaN layer in conventional LED structure. However, due to the lattice mismatch between GaN and $Al_XGa_{1-X}N$, there is a large polarization field in the last couple of quantum well (QW) and $Al_XGa_{1-X}N$ EBL, which will reduce the effective barrier height for electrons.[12] Thus, the electron leakage cannot be suppressed efficiently. On the other hand, the polarization field-induced band bending and the valence band offset (ΔE_v) at the interface of GaN and EBL will enhance the effective barrier height for holes and then slow down the hole injection.[5] Some methods of solving these problems have been proposed. Wang *et al.*[13] designed a grade-composition $Al_XGa_{1-X}N$ EBL (GEBL) to suppress the electron leakage and also to enhance the hole injection in simulation. Wang *et al.*[14] used sawtooth-shaped $Al_XGa_{1-X}N$–GaN–$Al_XGa_{1-X}N$ EBLs to enhance the electron confinement and the hole injection efficiency. Choi *et al.*[15] used InAlN with In composition 0.18, which is lattice-matched to GaN, as the EBL. Kuo *et al.*[16] used AlInGaN to replace the original EBL and barrier layer. Although using InAlN or AlInGaN as EBL can prevent the electron leakage effectively, the hole injection cannot be improved effectively due to the existence of high ΔE_v between the last GaN barrier and EBL.[12] In addition, it has been reported that p-AlGaN/GaN or p-InGaN/GaN superlattice (SL) in LED structure can prevent the carrier leakage over the EBL.[17,18] In this paper, we propose a new design that uses p-InGaN/AlInGaN SL as the EBL to prevent the carrier leakage over the EBL as well as to improve the hole injection efficiency. The electrical and optical properties of conventional LED with p-AlGaN EBL, LED with p-AlInGaN EBL, and LED with p-InGaN/AlInGaN SL EBL are investigated comparatively using APSYS simulation program developed by Crosslight Software Inc.[19]

2. Structure and parameters

Three LED samples were prepared on c-plane sapphire substrates, including a conventional LED with p-AlGaN EBL (labeled as sample A), an LED with p-AlInGaN EBL (labeled

*Project supported by the National Natural Science Foundation of China (Grant No. 51172079), the Science and Technology Program of Guangdong Province, China (Grant Nos. 2010B090400456 and 2010A081002002), and the Science and Technology Program of Guangzhou City, China (Grant No. 11A52091257).

†Corresponding author. E-mail: lishuti@scnu.edu.cn

© 2014 Chinese Physical Society and IOP Publishing Ltd

as sample B), and an LED with p-InGaN/AlInGaN SL EBL (labeled as sample C). Figure 1 shows the schematic layer structure of LED. First, a 20-nm thick low-temperature GaN nucleation layer, a 2.0-μm thick unintentionally-doped GaN (u-GaN) layer, and a 2.0-μm thick Si-doped (5×10^{18} cm^{-3}) n-GaN layer were sequentially deposited. Next, the active region consisted of six 3.0-nm thick InGaN quantum wells (QWs), separated by seven 10-nm thick GaN quantum barriers (QBs). On the top of the last QB was a total 20-nm thick Mg-doped (1×10^{18} cm^{-3}) EBL and a 170-nm thick Mg-doped (1×10^{18} cm^{-3}) p-GaN layer. The geometric size of the device was 300 μm×300 μm. The differences in EBL and their structure parameters among these three LEDs under study can be seen clearly from Table 1. Specifically, for sample A, the EBL with a total thickness of 20 nm is p-$Al_{0.2}Ga_{0.8}N$ layer. For sample B, the EBL with a total thickness of 20 nm is p-$Al_{0.2}In_{0.05}Ga_{0.75}N$ layer. For sample C, the EBL with a total thickness of 20 nm is composed of 4 periods of $In_{0.05}Ga_{0.95}N$ (2 nm)/$Al_{0.2}In_{0.05}Ga_{0.75}N$ (3 nm) SL layers. Most of the parameters used in this paper are the same as in Ref. [20]. The band gap energy parameters of the AlGaN, InGaN, and AlInGaN alloys can be found from Refs. [21] and [22].

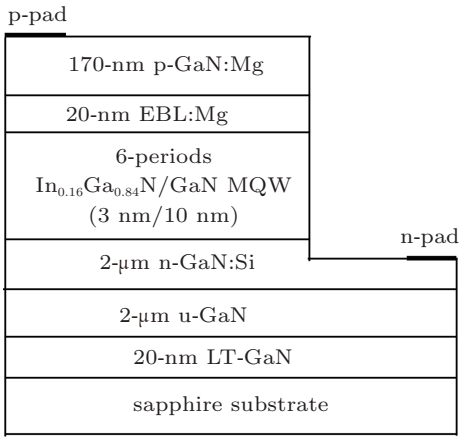


Fig. 1. Schematic structure of InGaN/GaN-based LED.

Table 1. Different EBLs and their structure parameters.

	EBL structure	Thickness
Sample A	$Al_{0.2}Ga_{0.8}N$	20 nm
Sample B	$Al_{0.2}In_{0.05}Ga_{0.75}N$	20 nm
Sample C	4 periods $In_{0.05}Ga_{0.95}N$/$Al_{0.2}In_{0.05}Ga_{0.75}N$ SLs	2/3/2/3/2/3/2/3 (total thickness=20 nm)

3. Results and discussion

Figures 2(a), 2(b), and 2(c) show the calculated energy band diagrams and quasi-Fermi levels of sample A, sample B, and sample C, respectively. The slope triangular barriers and wells, which are induced by the polarization field, can be seen clearly. Owing to the large spontaneous and piezoelectric polarizations, the energy band at the last-GaN-barrier/AlGaN-EBL interface in sample A is a downward slope (as shown in Fig. 2(d)), which reduces the potential barrier for electrons, and therefore augments the possibility for electrons to spill over the EBL to p-type region. In addition, the bend downward in the valence band of AlGaN EBL acts as a potential barrier for holes to be transported into the active region, and thus results in a poor hole injection efficiency. When AlInGaN is used as EBL in sample B, this phenomenon can be alleviated partly as shown in Fig. 2(e). Especially when InGaN/AlInGaN SL is used as EBL in sample C, this phenomenon almost disappears as shown in Fig. 2(f). The effective potential heights for electrons and holes in these three samples are also calculated. It can be found that the effective potential height for electrons in conduction band of sample A is the lowest in the three potential heights (i.e., 850 meV for sample A, 1028 meV for sample B, and 989 meV for sample C). This result implies the enhancements of electron confinement in sample B and sample C. Hence, more electrons can be blocked in the QWs and recombine with holes. On the other hand, the calculated effective potential height for holes in valence band of sample C is the lowest in the three potential heights (i.e., 820 meV for sample A, 761 meV for sample B, and 589 meV for sample C), which indicates the improvement of hole injection when InGaN/AlInGaN SL is used as EBL. It is worth noting that InGaN/AlInGaN SL EBL also introduces a series of potential wells causing holes to gather in the wells. The hole gathering will lead to a much larger hole concentration under the high injection current condition.[18] Schubert *et al.*[23] also theoretically suggested that the adoption of SL will enhance the acceptor activation by the modulation of the valence band, which will increase hole concentration and promote hole injection. Accordingly, InGaN/AlInGaN SL EBL in sample C can help to increase hole concentration, and therefore enhance hole injection compared with AlGaN EBL in sample A and AlInGaN EBL in sample B.

Owing to the large lattice mismatch between GaN, InGaN, and AlGaN, the electrostatic fields in the active region and at the interface of active region/AlGaN-EBL are very high, which can be seen form Fig. 3(a). It is evident that sample A possesses the largest electrostatic field near the last-barrier/EBL interface (i.e., 0.58 MV/cm), which leads to the band bending as discussed above. When AlInGaN or InGaN/AlInGaN SL is used as EBL, the polarization field is inhibited effectively, i.e., 0.1 MV/cm for sample B and 0.06 MV/cm for sample C. Because of the lower polarization field in the last-barrier/EBL interface, the band bending is alleviated (see Fig. 2(e) & Fig. 2(f)), thus the electronic leakage can be reduced and the hole injection efficiency can be enhanced. On the other hand, the InGaN/AlInGaN SLs in sample C introduce 0.4 MV/cm polarization field into the EBL region as can

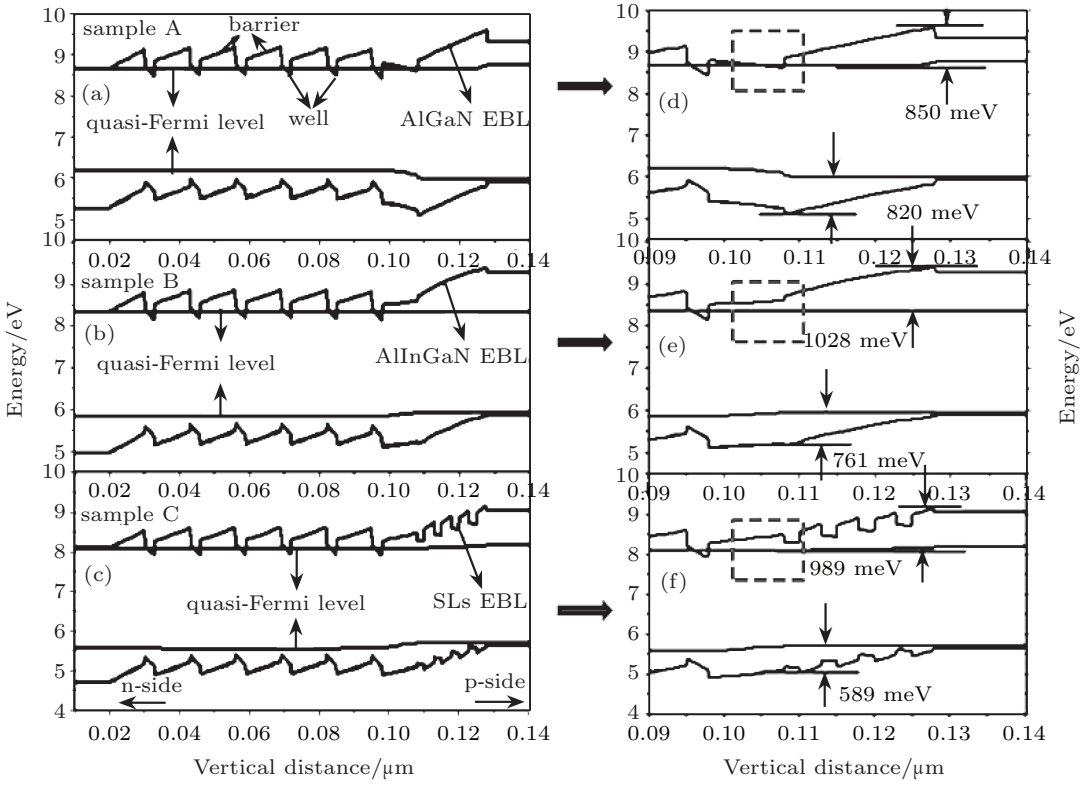


Fig. 2. Energy band diagrams of (a) sample A, (b) sample B, and (c) sample C. (d)∼(f) Enlarged last-barrier & EBL regions of sample A, sample B, and sample C, respectively.

be seen from Fig. 3(a). Simon *et al.*[24] have presented that Mg acceptor can be ionized by polarization field, so higher hole concentration can be expected in SL due to the polarization fields. Accordingly, hole injection can be promoted in sample C compared with in sample A and sample B. Figure 3(b) shows the current–voltage (I–V) characteristics of LED samples. Under an injection current of 20 mA, the forward voltages for sample A, sample B and sample C are 3.65 V, 3.53 V, and 3.46 V, respectively. The lower voltages in sample B and sample C, may be due to the higher hole injection efficiency.

Figures 4(a) and 4(b) show the simulated carrier concentrations of three LED samples in MQWs cut from n-side to p-side under an injection current of 50 mA. Note that the horizontal positions of sample B and sample C are shifted slightly for better observation. It can be seen clearly that a large number of carriers for all the samples accumulate in the last QW next to the p-type layer. From sample A to sample C, both electron concentrations and hole concentrations increase gradually. Especially in sample C, the total electron concentration increases about 24% and the total hole concentration increases about 28% compared with in sample A. These improvements of electron and hole concentrations can be attributed to the enhancements of hole injection efficiency and electron confinement. Figure 4(c) shows the radiative recombination rates of LED samples. It is obvious that most of the radiative recombinations happen in the QWs near the p-type layer. This is due to the non-uniform carrier distribution in QWs as discussed above. Besides, one can also find that the radiative

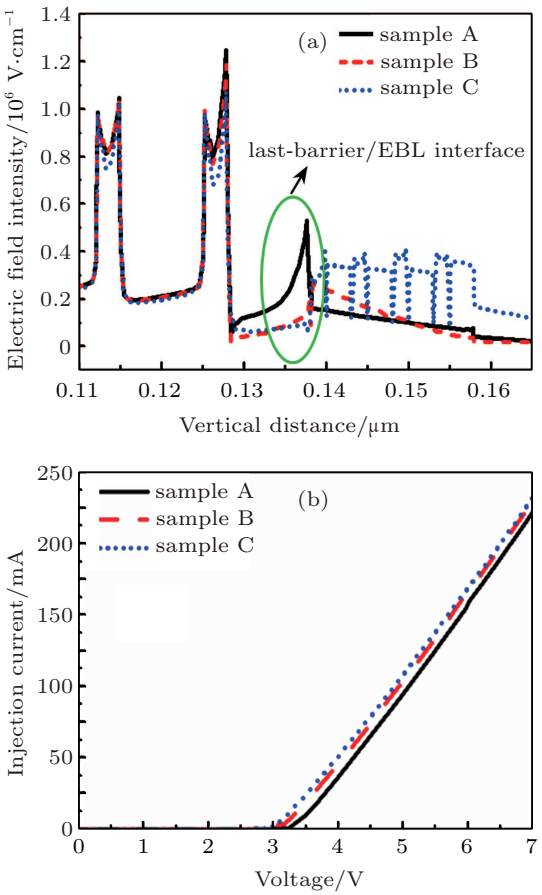


Fig. 3. (color online) (a) Electrostatic fields of these three LED structures; (b): Current–voltage performance curves of LED samples.

recombination rate for sample C is highest. This improvement in sample C is mainly attributed to its high electron and hole concentrations compared with those of sample A and sample B.

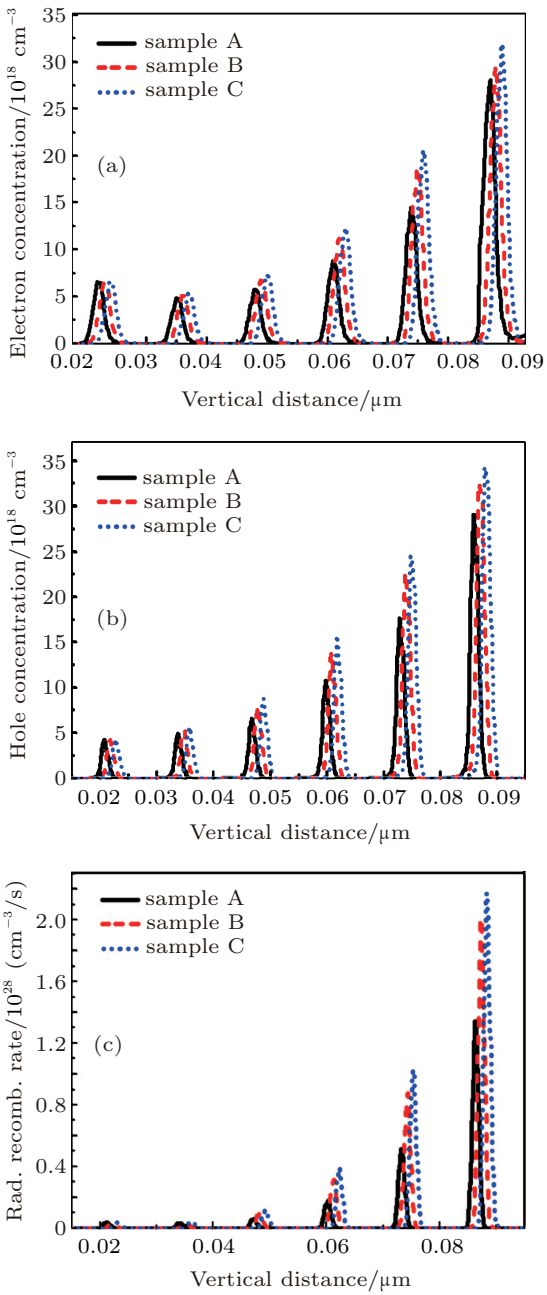


Fig. 4. (color online) Distributions of (a) electron concentrations, (b) hole concentrations, and (c) radiative recombination (rad. recomb.) rates of these three LED samples under an injection current of 50 mA.

Figure 5(a) shows the variations of electron current density with vertical distance of LED samples under 200 mA. One can find that the electron leakage current in sample A is severe, as high as 540 A/cm^2. When p-AlInGaN is used as EBL, the leakage can be alleviated partly. In our new design with p-InGaN/AlInGaN SL EBL, the leakage almost disappears. These results accord well with the above discussion. It is necessary to point out that even the electron effective potential height in sample C is a little lower than in sample B (see Figs. 2(e) and 2(f)), the electron leakage current is confined better. It can be attributed to the higher hole concentration in the active region of sample C than of sample B. Due to the increase of hole concentration in the quantum wells, more electrons can be recombined with holes in the active region, and accordingly the electron leakage can be reduced. The dependence of internal quantum efficiency (IQE) on forward current is presented in Fig. 5(b). With the increase of forward current, both sample A and sample B show obvious efficiency droop in IQE. In our new design for sample C, the efficiency droop can be effectively alleviated from 37.3% to 0.9% under 200 mA.

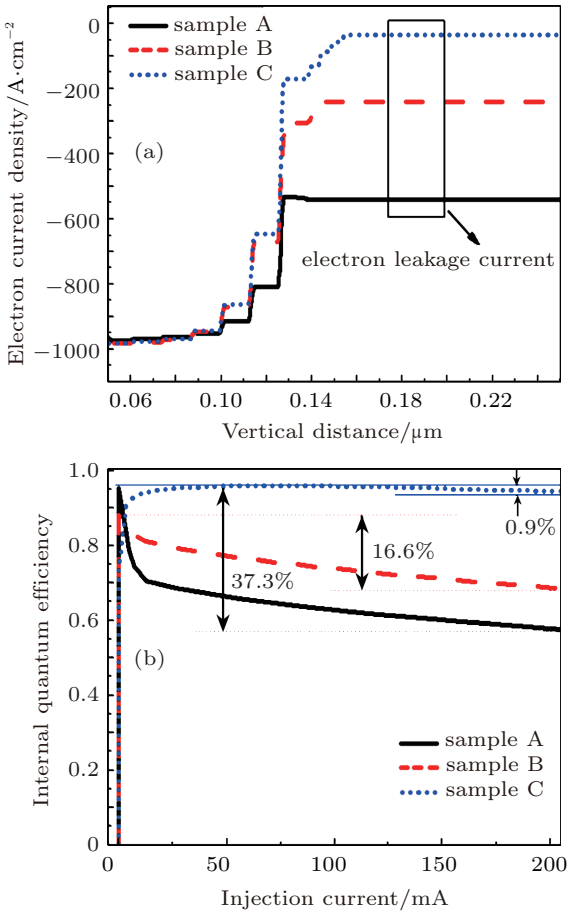


Fig. 5. (color online) (a) Electron current densities versus vertical distance and (b) IQEs versus injection current for these LED samples.

Figures 6(a) and 6(b) show the light–current (L–I) performance and the spontaneous emission spectra of LED samples, respectively. Both the light output power and the spontaneous emission rate in sample C are the highest, especially at high injection current. Because of the advantage in the alleviation of electron leakage to the p-side and the improvement of the hole injection efficiency, the performances of sample C with p-InGaN/AlInGaN SL EBL are shown to be superior to those of sample A and sample B, especially at high injection current.

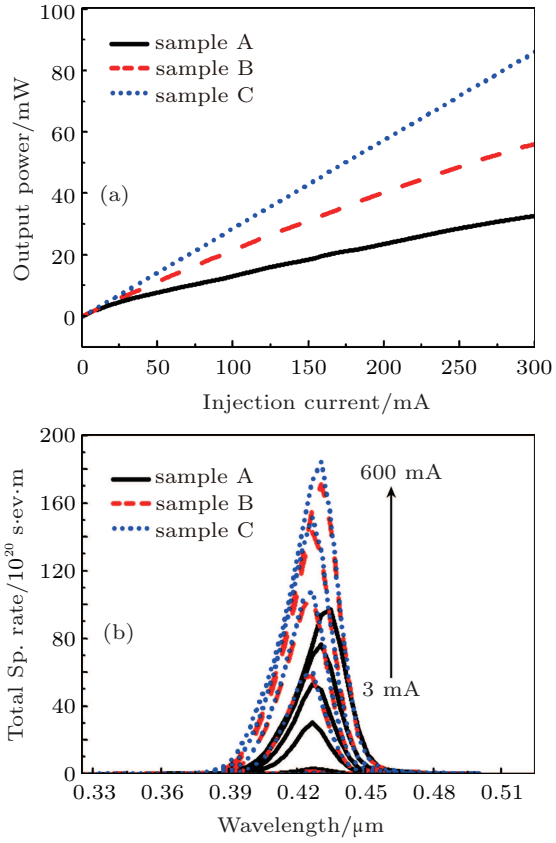


Fig. 6. (color online) (a) Light output versus current (L–I) characteristics and (b) calculated spontaneous emission spectra of the three LED samples.

4. Conclusions

In this paper, InGaN/GaN-based LEDs with p-AlGaN EBL, p-AlInGaN EBL, and p-InGaN/AlInGaN SL EBL are investigated comparatively using APSYS simulation program. It is found that the LEDs with traditional p-AlGaN EBL and p-AlInGaN EBL each show a low hole injection efficiency, severe electron leakage, and an inferior light output power with large efficiency droop at high injection current. In contrast, the LED with p-InGaN/AlInGaN SL EBL exhibits better optical and electrical performances such as higher light output power, higher IQE, and radiative recombination rate, lower forward voltage and current leakage. According to our numerical simulation and analysis, we attribute these improvements to the higher hole injection efficiency and better electron confinement when p-InGaN/AlInGaN SL is used as the EBL.

References

[1] Akyol F, Nath D N, Krishnamoorthy S, Park P S and Rajan S 2012 *Appl. Phys. Lett.* **100** 111118
[2] Ling S C, Lu T C, Chang S P, Chen J R, Kuo H C and Wang S C 2010 *Appl. Phys. Lett.* **96** 231101
[3] Shen Y C, Müller G O, Watanabe S, Gardner N F, Munkholm A and Krames M R 2007 *Appl. Phys. Lett.* **91** 141101
[4] Gardner N F, Müller G O, Shen Y C, Chen G, Watanabe S, Gotz W and Krames M R 2007 *Appl. Phys. Lett.* **91** 243506
[5] Kim M H, Schubert M F, Dai Q, Kim J K, Schubert E F, Piprek J and Park Y 2007 *Appl. Phys. Lett.* **91** 183507
[6] Tong J H, Li S T, Liu T P, Liu C, Wang H L, Wu L J, Zhao B J, Wang X F and Chen X 2012 *Chin. Phys. B* **21** 118502
[7] Xie J, Ni X, Fan Q, Shimada R, Ozgur U and Morkoc H 2008 *Appl. Phys. Lett.* **93** 121107
[8] Wu L J, Li S T, Liu C, Wang H L, Lu T P, Zhang K, Xiao G W, Zhou Y G, Zheng S W, Yin Y A and Yang X D 2012 *Chin. Phys. B* **21** 068506
[9] Monemar B and Sernelius B E 2007 *Appl. Phys. Lett.* **91** 181103
[10] Wang C H, Chen J R, Chiu C H, Kuo C H, Li Y L, Lu T C and Wang S C 2010 *IEEE Photon. Technol. Lett.* **22** 236
[11] David A, Grundmann M J, Kaeding J F, Gardner N F, Mihopoulos T G and Krames M R 2008 *Appl. Phys. Lett.* **92** 053502
[12] Han S H, Lee D Y, Lee S J, Cho C Y, Kwon M K, Lee S P, Noh D Y, Kim D J, Kim Y C and Park S J 2009 *Appl. Phys. Lett.* **94** 231123
[13] Wang C H, Ke C C, Lee C Y, Chang S P, Chang W T and Li J C 2010 *Appl. Phys. Lett.* **97** 261103
[14] Wang T H and Xu J L 2013 *Chin. Phys. B* **22** 088504
[15] Choi S, Kim H J, Kim S S, Liu J, Kim J, Ryou J H, Dupuis R D, Fischer A M and Ponce F A 2010 *Appl. Phys. Lett.* **96** 221105
[16] Kuo Y K, Tsai M C and Yen S H 2009 *Opt. Commun.* **282** 4252
[17] Gong C C, Fan G H, Zhang Y Y, Xu Y Q, Liu X P, Zheng S W, Yao G R and Zhou D T 2012 *Chin. Phys. B* **21** 068505
[18] Liu C, Li S T, Lu T P, Wu L J, Yin Y A, Xiao G W, Zhou Y G and Wang H L 2012 *IEEE Photon. Technol. Lett.* **24** 14
[19] See http://www.crosslight.com for more information about APSYS by Crosslight Software Inc., Burnaby, Canada
[20] Tong J H, Zhao B J, Wang X F, Chen X, Ren Z W, Li D W, Zhuo X J, Zhang J, Yi H X and Li S T 2013 *Chin. Phys. B* **22** 068505
[21] Bernardini F 2007 in *Nitride Semiconductor Devices: Principles and Simulation*, ed. Piprek J (New York: Wiley), p. 4968
[22] Vurgaftman I, Meyer J R and Ram-Mohan L R 2001 *J. Appl. Phys.* **89** 5815
[23] Schubert E F, Grieshaber W and Goepfert I D 1996 *Appl. Phys. Lett.* **69** 3737
[24] Simon J, Protasenko V, Lian C, Xing H and Jena D 2010 *Science* **327** 60